HMG Advance Access published April 7, 2016

Title page

Title

Identification of new molecular alterations in Fatal Familial Insomnia

Authors

Franc Llorens[1], Katrin Thüne[1], Matthias Schmitz[1], Belén Ansoleaga[2], Margalida A. Frau-Méndez[2], Maria Cramm[1], Waqas Tahir[1], Nadine Gotzmann[1], Sara Berjaoui[2], Margarita Carmona[2], Christopher J. Silva[3], Ivan Fernandez-Vega[4], Juan José Zarranz[5], Inga Zerr[1], Isidro Ferrer[2]*.

Affiliations

[1] Department of Neurology, University Medical Center Göttingen, and German Center for Neurodegenerative Diseases (DZNE)-site Göttingen, Göttingen, Germany

[2] Institute of Neuropathology, Service of Pathological Anatomy, Bellvitge University Hospital, University of Barcelona, Bellvitge Biomedical Research Institute (IDIBELL), Hospitalet de Llobregat, and Biomedical Research Center of Neurodegenerative Diseases (CIBERNED), Spain

[3] USDA, Produce Safety & Microbiology Research Unit, Western Regional Research Center, Albany, CA, USA

[4] Pathology Department University Hospital Araba, and Brain Bank Araba University Hospital, Basque Biobank for Research (O+eHun), Alava, Spain

[5] Neurology Department, University Hospital Cruces, University of the Basque Country, Bizkaia, Spain

Inga Zerr and Isidro Ferrer act as equivalent co-senior authors

Corresponding author:

Prof. Dr. Isidro Ferrer

Institute of Neuropathology, Service of Pathologic Anatomy, Bellvitge University Hospital,

Carrer Feixa Llarga sn, 08907 Hospitalet de Llobregat, Spain

Tel: +34 93 2607452

Fax: +34 93 4035808

Email: 8082ifa@gmail.com

Abstract

Fatal Familial Insomnia (FFI) is a rare disease caused by a D178N mutation in combination with methionine (Met) at codon 129 in the mutated allele of PRNP (D178N-129M haplotype). FFI is manifested by sleep disturbances with insomnia, autonomic disorders and spontaneous and evoked myoclonus, among other symptoms. The present study describes new neuropathological and biochemical observations in a series of eight patients with FFI. The mediodorsal and anterior nuclei of the thalamus have severe neuronal loss and marked astrocytic gliosis in every case, whereas the entorhinal cortex is variably affected. Spongiform degeneration only occurs in the entorhinal cortex. Synaptic and fine granular PrPres immunoreactivity is found in the entorhinal cortex but not in the thalamus. IL6, IL10RA, CSF3R and TLR7 mRNA expression increases in the thalamus in FFI. PrPc levels are significantly decreased in the thalamus, entorhinal cortex and cerebellum in FFI. This is accompanied by a particular PrPc and PrPres band profile. Altered PrP solubility consistent with significantly reduced PrP levels in the cytoplasmic fraction and increased PrP levels in the insoluble fraction are identified in FFI cases. Amyloid-like deposits are only seen in the entorhinal cortex. The RT-QuIC assay reveals that all the FFI samples of the entorhinal cortex are positive whereas the thalamus is positive only in three cases and the cerebellum in two cases. The present findings unveil particular neuropathological and neuroinflammatory profiles in FFI and novel characteristics of natural prion protein in FFI, altered PrPres and PrPsc patterns and region-dependent putative capacity of PrP seeding.

Introduction

Human prion diseases are classified as sporadic, iatrogenic or genetic according to the origin of the pathogenic prion protein. Mutations in *PRNP*, the gene encoding the prion protein, result in genetic (or familial) prion diseases including familial Creutzfeldt-Jakob disease (fCJD), Fatal Familial Insomnia (FFI) and Gerstmann-Sträussler-Scheinker disease (GSS). The clinical manifestations, neuropathology and prion species in these disorders largely depend on the site of the mutation and on the polymorphism at codon 129 in *PRNP* (1).

Fatal familial insomnia (FFI) is a fatal autosomal dominant prion disease caused by a *D178N* mutation in the *PRNP* in combination with methionine (Met) at codon 129 in the mutated allele of the same gene (*D178N-129M* haplotype) (2-5). The main clinical features of FFI include sleep disturbances with insomnia accompanied by autonomic disorders, hallucinations, delirium, and spontaneous and evoked myoclonus, among other symptoms (1,6-10). The age at onset and the duration of the disease are variable depending in part on the presence of methionine or valine at codon 129 in the normal allele of *PRNP* (1,9,11,12).

The most consistent morphological lesions are found in the mediodorsal and anterior thalamus which may extend to other thalamic nuclei. The inferior olives are also consistently affected. The entorhinal cortex is commonly involved but other brain regions are seldom affected in most cases. Neuron loss accompanied by dramatic astrogliosis without spongiosis is the most characteristic pattern in the thalamus and inferior olives whereas moderate neuron loss and astrocytic gliosis together with spongiosis predominate in the entorhinal cortex. Discrete loss of Purkinje cells can be found in the cerebellum and moderate astrogliosis without loss of neurons in the periaqueductal region (13-15). Neuroimaging studies of carriers have shown consistent hypometabolism in the thalamus even as an early sign of FFI (16). Immunohistochemistry reveals deposition of abnormal prion protein resistant to Proteinase K digestion (PrPres) in the entorhinal cortex while in the thalamus, PrPres is absent, or present in very low amounts, thus suggesting a lack of relation between PrPres, neuron loss and astrocytic gliosis in FFI (17-19). Microglial activation in the thalamus is apparently discrete in FFI (20,21). The molecular mechanisms involved in FFI pathogenesis are poorly documented. There is altered regulation of transcription, protein biosynthesis, protein folding, protein transport, RNA

splicing, the electron transport chain, oxidative phosphorylation, energy metabolism, transport, and oxidation reduction (22,23). Proteomic studies have also revealed altered profiles in the neocortex in FFI (24). Unfortunately, the thalamus was not examined in that study. Recently, we described marked alterations in the expression of molecules linked to energy metabolism and to protein synthesis in the mediodorsal thalamus in FFI (Frau-Mendez *et al.,* submitted).

Transgenic models carrying the D178N mutation have been useful to learn about the effects of this mutation in brain as lesions are reminiscent of those seen in FFI despite conflicting data regarding the generation of transmissible prions (25,26).

The present study analyses pathological and molecular features in the brains of eight FFI patients who carried the D178N mutation and were Met/Met homozygous at codon 129 of *PRNP*. Special attention was paid to neuropathological and biochemical markers of neurons, astrocytes and microglia, inflammatory responses, characteristics of the natural FFI-prion protein, and pathological-prion (PrPres and PrPsc) species in FFI.

Results

1. Neuronal changes

Severe neuron loss without accompanying spongiosis was seen in the mediodorsal and anterior thalamus, and inferior olive in every case; neuron loss was variable from severe to marked in the pulvinar. Moderate neuron loss with spongiosis in the entorhinal cortex occurred in all but one case. Purkinje cell loss was discrete and focal (Figure 1).

Protein expression of the presynaptic markers synapsin and synaptophysin, and postsynaptic PSD-95, were reduced in the thalamus and entorhinal cortex in FFI, whereas only moderate reduction of PSD-95 loss was found in the cerebellum (Figure 2A and B). Levels of 14-3-3 isoforms γ, β and ε were similar in control and FFI cases (Figure 2A and B). Neuronal marker NeuN and low molecular weight neurofilament protein (NFL-L) levels were markedly reduced in the thalamus and entorhinal cortex in FFI but unaltered in the cerebellum (Fig. 2A and B). Protein levels of total Tau and phospho-Tau (p-Tau) were reduced in the three regions in FFI (Fig 2A and B). Decreased Tau protein levels were associated with decreased RNA expression levels in the thalamus and entorhinal cortex in FFI (Figure 2C).

2. Glial changes

A marked increase in GFAP mRNA expression and immunoreactivity, as revealed by immunohistochemistry and Western blotting, was observed in the thalamus, entorhinal cortex and cerebellum in FFI (Figure 3A, B and C). No major alterations in Iba-1 (protein and mRNA) and Cd11b and Cd68 (mRNA) expression were observed in FFI, except two cases which showed a marked increase in the three microglial markers with RT-qPCR analysis in the thalamus (Figure 3A, B and C) and in one case in the cerebellum that showed increased Iba-1 expression with Western blotting. No modifications in Olig2, used as an oligodendrocyte marker, and the dual astroglia and microglia activator CNTF mRNA expression levels, were seen in any region in FFI when compared with controls (Figure 3A).

3. Inflammatory markers

Seventeen mRNAs encoding pro- and anti-inflammatory cytokines, toll-like receptors, colony stimulating factors, cathepsins and members of the complement system, were assessed in FFI and

control cases. Increased expression of interleukin 6 (*IL6*), interleukin 10 receptor alpha subunit (*IL10RA*), colony stimulating factor 3 receptor (*CSF3R*) and toll-like receptor 7 (*TLR7*) was found in the thalamus in FFI (Table 1A). In contrast, interleukin 10 (IL10) was downregulated in the entorhinal cortex in FFI compared with controls (Table 1B).

IL6 mRNA upregulation in the thalamus was validated using two additional housekeeping genes (GAPDH and GUSB) (Figure 4A). IL6 protein is expressed in reactive microglia in the entorhinal cortex and the thalamus in FFI (Figure 4B).

Regarding inflammatory pathways and mediators, expression levels of IkBα were diminished in the thalamus and entorhinal cortex, but not in the cerebellum in FFI. This was accompanied by increased expression of the phosphorylated band (appears as a doublet) (Figure 4C). The expression of superoxide dismutase 1 (SOD1) was also increased in the thalamus and entorhinal cortex, whereas elevated cyclooxygenase 2 (COX-2) expression levels were only detectable in the thalamus in FFI (Figure 4C).

4. PrP expression

Brain extracts of control and FFI cases were analysed for PrP levels using a battery of antibodies mapping to different epitopes of the PrP sequence to exclude epitope-dependent bias (Figure 5A). PrP levels were significantly decreased in the thalamus, entorhinal cortex and cerebellum in FFI compared with controls, as revealed by densitometric analysis of Western blot bands (Figure 5B and C). However, increased expression of the nonglycosylated band of about 19 kDa was observed in the thalamus when using PrP antibodies mapping to the central region of PrP comprising the α-helical domains H1 and H2 (Figure 5B). Decreased PrP mRNA levels are also observed in the thalamus and entorhinal cortex in FFI cases (Figure 5C).

5. Analysis of abnormal PrP forms

Western blot analysis with SAF70 antibody of PK-digested FFI brain homogenates revealed that the diglycosylated PrPres band was the most abundant, followed by the monoglycosylated form, whereas the nonglycosylated band of about 19 kDa was under-represented in the entorhinal cortex in FFI cases. In contrast, no PK-resistant PrP was detected in the thalamus and cerebellum (Figure 6A). PrP immunohistochemistry using the 3F4 antibody showed synaptic and fine granular PrPres

immunoreactivity in the entorhinal cortex while no PrP signal was detected in the thalamus (Figure 6B) and cerebellum (data not shown) (Figure 6B).

In order to detect conformational modifications of PrP, dot blot analysis using the anti-PrP conformational antibody 15B3 was performed in FFI and control cases. Increased signal was observed in the entorhinal cortex and to a lesser degree in the thalamus in FFI cases when compared to controls. The signal was lower than that observed in the cerebellum from a sCJD MM1 case that was used as a positive control. Densitometric analysis showed significant differences between control and disease cases ($p<0.01$ and $p<0.001$, respectively for the thalamus and entorhinal cortex) and between the entorhinal cortex and thalamus in FFI cases ($p<0.05$) (Figure 7A).

As an alternative method to assess the levels of abnormal PrP, brain homogenates of control, FFI and sCJD cases were incubated with Ac-NHS, a compound that acetylates the ε-amino group of lysines. The epitope of the 3F4 antibody contains a lysine. If that lysine is acetylated, then the 3F4 antibody will no longer recognize that now acetylated epitope and will not bind to PrP. When PrP is in the PrPc conformation the lysine of the 3F4 epitope is available to react with the reagent and is entirely acetylated. This results in the elimination of signal from 3F4, since the 3F4 epitope has been acetylated and is, therefore, no longer present in PrP (Figure 7B). When PrP is in the PrPsc conformation, the lysine of the 3F4 epitope is hidden and less available to react with Ac-NHS, which means that the lysine of the 3F4 epitope is unacetylated and can be recognized by the 3F4 antibody (27). As expected, incubation of control cases with Ac-NHS completely abrogated the signal detectable with 3F4 (Figure 7B). Incubation of sCJD with Ac-NHS slightly decreased the detectable signal with 3F4. Quantification of signal intensities with and without Ac-NHS treatment showed that 66.2 ± 19% of all PrP in the frontal cortex of sCJD is in the form of a misfolded PrP not able to react with Ac-NHS. However, incubation of FFI with Ac-NHS showed that only 9.1 ± 7.4% was abnormal PrP, whereas no signal was identified in the thalamus after Ac-NHS (Figure 7B).

6. PrP solubility and detection of oligomeric and amyloid forms

PrP solubility was assessed in samples of the thalamus and entorhinal cortex in FFI cases compared with controls. Cytoplasmic (PBS-soluble), membrane (deoxycholate-soluble) and insoluble (SDS-soluble) fractions were processed for Western blotting with the SAF70 antibody. Diglycosylated and

monoglycosylated forms predominated in the membrane followed by the insoluble fraction in control and FFI samples (Figure 8A). A small amount of PrP was also detected in the cytoplasmic fraction. However, altered solubility was observed in FFI compared with controls. Significantly reduced levels of PrP ($p<0.05$) in the cytoplasmic fraction and increased levels of insoluble PrP ($p<0.05$) were found in FFI cases when compared with controls (Figure 1A). The same pattern was seen in the frontal cortex and cerebellum in sCJD MM1 when analysed in parallel with a corresponding control used for comparison ($p<0.01$ and $p<0.001$, respectively, for the cytoplasmic and insoluble fractions) (Figure 1A, only frontal cortex shown).

To further characterise the presence of misfolded structures, we analysed for the presence of oligomers. Dot blot analysis of FFI and sCJD MM1 brain homogenates using the anti-oligomer antibody 11A indicated the presence of oligomeric species in the thalamus of FFI cases but in smaller amounts than those detectable in the cerebellum of sCJD (Figure 8B).

Presence of amyloid-like structures in FFI cases was assessed by incubation of brain homogenates with thioflavin T (ThT) followed by quantification of the fluorescence signal. A significant increase in ThT signal was detected in the entorhinal cortex of FFI cases compared with controls ($p<0.05$). Although a similar trend was also observed in the thalamus, these samples showed high variability. In contrast, high ThT binding to amyloid structures was observed in the cerebellum in sCJD MM1 used as a positive control ($p<0.001$) but not in the cerebellum of FFI (Figure 8C).

7. PrP seeding activity

Due to the low amounts of pathogenic-related PrP forms detected in the brains of these FFI cases, we tested the ability of these forms to act as seeds for non-pathogenic PrP using the RT-QuIC assay, which mimics *in vitro* the conversion of PrPc to misfolded and amyloid PrP (28-30).

Brain homogenates were diluted from 10^{-3} to 10^{-8} in order to find the optimal range of detection. At a dilution of 10^{-8} all the FFI samples of the entorhinal cortex were positive whereas the thalamus was positive only in three of seven FFI cases; the cerebellum was positive in two of eight cases (Figure 9A). All controls were negative at all dilutions (data not shown).

Significant correlation was detected between the levels of PrPres (quantified from PK-digestion experiments) and RT-QuIC signal in the entorhinal cortex (Figure 9B), while no correlation between

total PrP (quantified from SAF70 Western blot) and RT-QuIC signal was observed in the same region (Figure 9B). Since no positive PrPres was previously detected in the thalamus and cerebellum of FFI cases, correlations in these brain regions cannot been established.

To quantify the regional and prion disease differences in seeding activity, 10^{-6} brain homogenate dilutions (for which all prion cases were positive) of the thalamus, entorhinal cortex and cerebellum of FFI cases, and frontal cortex and cerebellum of sCJD, were analysed in parallel (Figure 10A). The RT-QuIC signal was quantified using the area under the curve (AUC) (cumulative measurement of seeding efficiency) and lag phase (time to reach 10,000 RFU) parameters. The thalamus and entorhinal cortex of FFI cases, and the frontal cortex and cerebellum of sCJD cases, showed similar seeding ability considering AUC and lag phase. However, the cerebellum of FFI cases showed increased lag phase and decreased AUC values, indicating less seeding activity (Figure 10B and C).

A general overview of the major findings is presented in Supplementary Table 3.

Discussion

1. Neuropathological observations

Relative homogeneity of lesions in the present series can be related, at least in part, to the homozygosity Met/Met in all cases. All FFI cases were males, had the *D178N* mutation and were met/met homozygous at codon 129 of *PRNP*. Regarding the three regions analysed, marked neuronal loss and severe astrocytic gliosis without spongiosis were found in the thalamus, especially in the mediodorsal nucleus; moderate neuron loss, astrocytic gliosis and spongiosis in the entorhinal cortex in most cases; and focal Purkinje cell loss and astrocytic gliosis without spongiosis in the cerebellum in some cases, as already reported (15,31). PrPres deposition was detected by immunohistochemistry in the entorhinal cortex in the present cases. Morphological alterations were accompanied by biochemical evidence of reduced neuronal and synaptic markers, including neurofilaments, NeuN, synapsin, synaptophysin, PSD-95, Tau and phospho-Tau, particularly in the thalamus and entorhinal cortex, together with increased expression levels of glial fibrillary acidic protein used as a marker of astroglia. Interestingly, although variable from one to the other, 14-3-3 levels in FFI brains do not differ from controls, in agreement with the absence of 14-3-3 in the CSF of FFI cases (32). The presence of PrPres in the entorhinal cortex correlates with spongiosis as already reported in human and animal prion diseases (33). This does not mean a close causative relationship as PrPres is also detectable in regions where no major lesions are present, and similar amounts of PrPres are found in regions with distinct vulnerability (34). No correlation between abnormal PrP deposition, loss of synapses and neurological deficits has been observed in human and animal prion diseases (35-37).

2. Inflammatory profiles in FFI

The observation of limited activated microglia in the three brain regions analysed in FFI is in agreement with a report of a small cohort of FFI cases where Iba-1 was used as a microglial marker (20). However, microglial activation, as demonstrated by expression of the class II major histocompatibility Human Leukocyte Antigen-DR (HLA-DR), has been reported in the thalamus in FFI (21).

The quantitative methods used in the present study have shown non-altered expression levels of different microglial markers (Iba-1, Cd11b and CD68), together with increased expression of IL6,

IL10RA, CSF3R and TLR7 in the thalamus in FFI, which explains the seemingly contradictory results of the previous studies. Increased numbers of activated microglia are found in the thalamus in two cases. Although gene upregulation of cytokines and mediators of the immune response in FFI is far from the dramatic deregulation in sCJD (38), the present findings indicate minor but significant inflammatory responses in the thalamus in FFI. IL6 triggers COX-2 expression (39), suggesting a regional-dependent activation of IL6-COX-2 signaling in the thalamus in FFI. Indirect evidence of activation of the NFκB is in agreement with observations in scrapie-infected mice (40) and in sCJD (38,41).

Elevated SOD-1 levels in thalamus and entorhinal cortex regions argue in favor of oxidative stress responses in FFI such as those seen in human and animal prion diseases (38,42,43) are not available in FFI.

3. Particular PrP species in FFI

Decreased PrP mRNA and protein expression levels have been reported in the frontal cortex of sCJD MM1 cases and in the cerebellum of sCJD VV2 samples (44), and in the neocortex of sCJD mice tg340-129MM carrying the human PrP gene (38). The present study shows that PrP mRNA and protein levels are also reduced in the thalamus and entorhinal cortex in FFI. Low levels of abnormal PrP and PrPres in FFI cases are also in line with downregulation of PrPc in FFI.

In agreement with seminal descriptions, the diglycosylated PrP band is the most abundant form, followed by the monoglycosylated form in the thalamus, entorhinal cortex and cerebellum in FFI, whereas the nonglycosylated form is underrepresented (10,17,45). However, a robust nonglycosylated band of about 19 kDa is observed in the thalamus of FFI cases using antibodies against the H1 and H2 regions of prion protein. Different prion strains present specific glycosylation patterns (46,47), and PrP glycosylation display strain-specific properties (45,48). These characteristics seem to have implications in the modulation of PrP conversion (49). The presence of this unique band in the thalamus suggests that specific prion species or strains are expressed in this region in FFI. Whether this has implications in the major vulnerability of the thalamus in FFI is not known.

4. Conformational modifications of PrP in FFI

PrPres typing in the entorhinal cortex in the present series is characteristic of 19 kDa PrPsc type 2 with underrepresentation of the nonglycosylated form and increased expression of the diglycosylated band (4,17). The present observations also show altered conformation and solubility of PrP, as well as the presence of oligomers in the thalamus and entorhinal cortex in FFI similar to that seen in sCJD. However, the proportion of total PrP versus PrPres is higher in FFI when compared with sCJD thus explaining, in part, the almost negligible low amount of PrPres in some cases, in the thalamus in FFI (17).

5. Toxic species and seeding capacity of PrP in FFI

The precise nature of the PrP species responsible for toxicity in FFI needs to be deciphered although the present data suggest that oligomers and amyloid aggregates are certainly not the most abundant components of PrP species in FFI. This is in contrast with evidence showing oligomeric species as the main toxic and infective agent in prion disease models (50-52). In parallel, the present findings also suggest that PrPres is not the only actor in prion disease pathogenesis (53-57).

Additionally, the present findings show that PrP from FFI cases has seeding capacities similar to those of sCJD as revealed by RT-QuIC analysis. Although the correlation between *in vitro* seeding assays and true *in vivo* propagation and transmissibility of misfolded PrP remains to be elucidated, the high seeding activity of the thalamus and entorhinal cortex suggests that PrP in FFI has the capacity to induce *de novo* misfolded PrP molecules even considering a scenario with low, almost absent, PrPres levels, as in the thalamus.

Following a recently suggested definition of infection, considered as a process by which a self-propagating agent causes disease or damage as a consequence of its intrinsic capacity to make identical or similar copies of itself through a diversity of mechanisms requiring, or not, an exogenous component (58), FFI-PrP has infective properties *in vitro* similar to other prion strains while presenting different molecular, biophysical and biochemical properties. However, since FFI brain tissue has low infectivity in classical prion bioassays, it may be speculated that this effect in natural conditions is restricted to vulnerable brain regions and depends on the particular characteristics of the host's prion (i.e., specific mutation of the prion protein). Yet spontaneous generation of prion infectivity has been reproduced in FFI knock-in mice (26).

Material and Methods

Cases and general processing

All the cases were from the Basque Country in the north of Spain where FFI has a relatively high incidence due to a founder effect in a historically small rural community with endogamy not uncommon (59).

Brain tissue was obtained from the Institute of Neuropathology Biobank and the Brain Bank of the Araba University Hospital and Basque Biobank for Research (O+eHun) following the guidelines of the Spanish legislation on this matter and the approval of the local ethics committees. The post mortem interval between death and tissue processing was between 2 h and 22 h 50min. One hemisphere was immediately cut in coronal sections, 1cm thick, and selected areas of the encephalon were rapidly dissected, frozen on metal plates over dry ice, placed in individual airtight plastic bags, numbered with water-resistant ink and stored at -80ºC until use. The other hemisphere was fixed by immersion in 4% buffered formalin for 3 weeks. Neuropathological examination in all cases was routinely performed on twenty selected de-waxed paraffin sections comprising different regions of the cerebral cortex, diencephalon, thalamus, brain stem and cerebellum, which were stained with hematoxylin and eosin, Klüver-Barrera and for immunohistochemistry to microglia, glial fibrillary acidic protein, β-amyloid, phosphorylated Tau (clone AT8), α-synuclein, TDP-43, ubiquitin, PrP (3F4 antibody) and p62. FFI cases (n = 8) were genotyped and identified, all of them, as carriers of the *D178N* mutation *in PRNP* and M/M at codon 129 of the same gene. Age-matched control cases (n = 9) had not suffered from neurologic or psychiatric diseases or, metabolic disorders (including metabolic syndrome), and did not have abnormalities in the neuropathological examination excepting sporadic Alzheimer's disease-related pathology stages I-II/0 of Braak and Braak. In addition to these controls, cases of sCJD subtype MM1 (n = 4) were used for comparative studies of PrP. Morphological and biochemical studies were centered on the thalamus, entorhinal cortex and cerebellum.

Antibodies and reagents

Anti-β-actin (1:10,000) was from Sigma (St. Louis, MO, USA) and anti-Tau (N-ter) (1:1,000) from Millipore (Temecula, CA, USA). Anti-p-Tau (T181) (1:1,000) was from Calbiochem (San Diego, CA, USA), anti-14-3-3 isoforms (1:2,000) from Santa Cruz Biotechnology (Santa Cruz, CA, USA), anti-synaptophysin (1:5,.000) and anti-SOD1 (1:2.000) from Novocasta-Leica (Wetzlar, GE), anti- post-synaptic density protein 95 (PSD-95) (1:1.000), anti-synapsin (1:2.000) and anti-IκBα (1:1.000) from Cell Signaling Technology (Beverly, MA, USA), anti-neuronal nuclei (NeuN) from Chemicon-Millipore (Temecula, CA, USA), anti Neurofilament Light (NF-L) (1:5.000) and anti-GFAP (1:5.000) from Dako (Santa Clara, CA, USA), anti-Tau (Tau-5) (1.1.000) from Thermo Scientific (Wilmington, DE), and GAPDH (1:2.000) from Abcam (Cambridge, UK). Anti-COX-2 (1:1.000) was from Cayman (Ann Arbor, MI, USA) and anti-Iba-1 (1:1.000) from Wako (Richmond, VA, CA). 15B3 (1:1.000) was from Prionics (Schlieren, SW). Anti-oligomer antibody (11A) (1:2000) was from Invitrogen (Waltham, MA, USA). Anti PrP antibodies (1:1000) were from Cayman (SAF32, SAF61 and 12F10), Abcam (8H4) and Millipore (3F4). Proteinase K (PK) and Thioflavin-T (ThT) were from Sigma.

Western blotting

Human tissues were lysed in lysis buffer containing 100mM Tris pH 7, 100mM NaCl, 10mM EDTA, 0.5% NP-40 and 0.5% sodium deoxycolate plus protease and phosphatase inhibitors. After centrifugation at 14,000g for 20 min at 4°C, supernatants were quantified for protein concentration with Bradford reagent (Bio-Rad, Hercules, CA, USA), mixed with SDS-PAGE sample buffer, boiled and subjected to 8–15% SDS-PAGE. Gels were stained with Coomassie or transferred onto polyvinylidene difluoride membranes and processed for specific immunodetection using electrochemiluminescence reagent. For the detection of PrP, a buffer containing 100mM Tris pH 7, 100mM NaCl, 10mM EDTA and 0.5% SDS plus protease and phosphatase inhibitors was used in parallel to detect differences in the amount of insoluble PrP extracted from brain tissues. Using different detergent composition, no differences in the PrP western blot patterns or expression levels were detected (data not shown).

Proteinase K digestion

10% w/v brain tissue homogenates were incubated with different proteinase K (PK) concentrations (25-100 μg/ml) for 1h at 37°C. Reactions were stopped with 1mM Phenylmethylsulfonyl fluoride and developed for Western blot with anti-PrP antibodies.

RNA purification and reverse transcription

RNA was obtained from entorhinal cortex and dorsomedial thalamus of FFI cases and controls using RNeasy Lipid Tissue Mini Kit (Qiagen Hilden, GE) following the instructions of the supplier. RNAs were treated with DNase Set (Qiagen) for 15 min to eliminate genomic DNA contamination. The concentration of each sample was measured using a NanoDrop 2000 spectrophotometer (Thermo Scientific) at 340nm. RNA integrity was assessed with the RNA Integrity Number (RIN value) determined with the Agilent 2100 Bioanalyzer (Agilent, Santa Clara, CA, USA). RIN values are shown in Table I. Reverse transcriptase reaction was carried out with the High Capacity cDNA Archive kit (Applied Biosystems Foster City, CA, USA). RNA from cerebellum in FFI cases did not of sufficiently high quality and therefore the cerebellum was not included in mRNA studies.

qPCR

Quantitative RT-qPCR assays were performed in duplicate on cDNA samples obtained from the retro-transcription reaction diluted 1:20 in 384-well optical plates (Kisker Biotech Steinfurt, GE) using the ABI Prism 7900 HT Sequence Detection System (Applied Biosystems). The reactions were carried out using 20xTaqMan Gene Expression Assays for genes involved in protein synthesis, energetic metabolism and purine metabolism, and 2xTaqMan Universal PCR Master Mix (Applied Biosystems). TaqMan probes are shown in Supplementary Table 2.

The reactions were conducted following the parameters: 50ºC for 2 min, 95ºC for 10 min, 40 cycles at 95ºC for 15 sec and 60ºC for 1 min. The fold change was determined using the equation 2-ΔΔCT.

RT-QuIC

RT-QuIC was performed as described previously (25) with minor modifications. Briefly, 85μl of reaction buffer was seeded in the presence of recombinant PrP (10μg) with 15μl of 10%w/v brain homogenates. Tissues were lysed in PBS 0.1% SDS and clarified by centrifugation for 10min at 10,000g and further diluted from 10^{-3} to 10^{-8} in PBS. Reaction was set in a final volume of 100μl and placed in a 96-well black optical bottom plate (Fisher Scientific). Each sample was run in duplicate.

Prepared plates were sealed and incubated in a FLUO Star OPTIMA plate reader (BMG Labtech Ortenberg, GE) at 42°C for 80 h with intermittent shaking cycles, consisting of one minute double orbital shaking at the highest speed (600rpm) followed by a one minute break.

All RT-QuIC experiments were performed using the chimeric recPrP composed of the Syrian hamster residues 14 to 128 followed by sheep residues 141 to 234 of the R154 Q171 polymorphic haplotype as described elsewhere (60).

Immunohistochemistry

4 µm-thick de-waxed paraffin sections were treated to block endogenous peroxidases followed by 10% normal goat serum. After incubation with appropriate antibodies, the sections were incubated with EnVision+ system peroxidase (Dako) at room temperature for 15 min. The peroxidase reaction was visualized with diaminobenzidine and H_2O_2. The omission of the primary antibody in some sections was used as a control of immunostaining; no signal was obtained with incubation of only the secondary antibody. Sections were slightly counterstained with hematoxylin.

Amyloidogenic and oligomeric PrP analysis

For dot blot analysis of PrP, 10% w/v brain homogenates were prepared in lysis buffer containing PBS, 0.5% Nonidet P-40, 0.5% deoxycholate, and protease and phosphatase inhibitors. After clarification of the homogenates, the supernatants were diluted 1:25 and loaded on 0.2µm nitrocellulose membranes using a dot blot system (Bio-Rad). The membranes were blocked with 5% (w/v) non-fat dry milk in Tris-buffered saline/Tween 20 (TBS-T) for 1 hour at room temperature and then incubated with primary antibodies overnight at 4°C. 15B3 antibodies were used for the detection of PrP conformation, and the anti-oligomer antibody clone A11 for the detection of PrP oligomeric forms.

For ThT staining, brain homogenates were prepared in lysis buffer containing PBS, 0.5% Nonidet P-40, 0.5% deoxycholate, and protease and phosphatase inhibitors. Samples were diluted 1:20 in PBS, mixed with ThT at a final concentration of 20 □M and incubated for 10 min with gentle shaking at room temperature. Beta-sheet formation kinetics was determined by measuring ThT fluorescence signal (450nm excitation and 480nm emission) every 30 min expressed in relative fluorescence units (RFU).

PrP quantification

Ten µL brain homogenate (10% w/v), 4.4 µL octyl β-D-glucopyranoside (20% w/v in water) and 4.4µL sodium phosphate (pH 8.0) were mixed before adding 4.4 µL of a dimethylsulfoxid (DMSO) solution containing the N-hydroxysuccinimide ester of acetic acid (Ac-NHS) (0µM to 50µM), and incubated with continuous rotation for 15 min at room temperature. Afterwards, 4.4µL 1M Tris buffer (pH 8.0) was added and the reaction was incubated in a rotator for another 15 min at room temperature. The analysis was carried out with by Western blot using the 3F4 antibody. Under these assay conditions, 10µm Ac-NHS final concentration showed a complete removal of electrochemiluminescence signal in control brains while PrPsc was still detectable in prion-infected brain samples.

PrP solubility

Solubility of PrP in different detergents was assessed as detailed elsewhere (61) with minor modifications. Brain samples (50mg) of entorhinal cortex and thalamus from control and FFI cases (n=3 for each region and group) were homogenised in a Polytron homogeniser in 750µL of ice-cold PBS+ (sodium phosphate buffer pH 7.0, plus protease inhibitors) and centrifuged at 5,200 rpm at 4°C for 10 min. The pellet was discarded and the resulting supernatant was centrifuged at 16,500g at 4°C for 90 min. The supernatant (S2) was kept as the PBS-soluble fraction. The resulting pellet was resuspended in a solution of PBS, pH 7.0, containing 0.5% sodium deoxycholate, 1% Triton, and 0.1% SDS, and this was centrifuged at 16,500g at 4°C for 90 min. The resulting supernatant (S3) was kept as the deoxycholate-soluble fraction. The corresponding pellet was resuspended in a solution of 2% SDS in PBS and maintained at room temperature for 30 min. Afterwards, the samples were centrifuged at 16,500g at 25°C for 90 min and the resulting supernatant (S4) was the SDS-soluble fraction. Fractions were analysed by Western blotting with anti-PrP antibodies.

Statistical analysis

ANOVA test followed by Tukey's Multiple-Comparison post hoc test was used to compare the values from the different groups. Unpaired two-tailed t-test was used for the comparison of two groups of samples. Values were expressed as mean ± SD. Values considered significant were represented as *p

< 0.05; ** $p < 0.01$ and *** $p < 0.001$. Statistical analysis was carried out using Graph Pad Prism 6 software.

Acknowledgments

This study was funded by the Seventh Framework Program of the European Commission (Grant No. 278486 [DEVELAGE project]) and by the Spanish Ministry of Health, Instituto Carlos III (Fondo de Investigación Sanitaria [FIS] PI1100968, FIS PI14/00757, and CIBERNED project BESAD-P to Isidro Ferrer , by the European Commission: Protecting the food chain from prions: shaping European priorities through basic and applied research (PRIORITY, N°222887) Project number: FP7-KBBE-2007-2A, the Neurodegenerative Disease Research (JPND-DEMTEST: Biomarker based diagnosis of rapidly progressive dementias-optimization of diagnostic protocols, 01ED1201A) to Inga Zerr, and to the Red Nacional de priones (AGL2015-71764-REDT- MINECO) to Isidro Ferrer, Franc Llorens and Inga Zerr. We wish to thank T. Yohannan, Mohsin Shafiq and Melissa Erickson-Beltran for editorial help.

Conflict of Interest

The authors declare that there are no conflicts of interest.

References

1. Capellari,S., Strammiello,R., Saverioni,D., Kretzschmar,H., Parchi,P. (2011) Genetic Creutzfeldt-Jakob disease and fatal familial insomnia: insights into phenotypic variability and disease pathogenesis. *Acta Neuropathol.*, **121**, 21-37.

2. Medori,R., Tritschler,H.J. (1993) Prion protein gene analysis in three kindreds with fatal familial insomnia (FFI): codon 178 mutation and codon 129 polymorphism. *Am. J. Hum. Genet.*, **53**, 822-827.

3. Medori,R., Tritschler,H.J., LeBlanc,A., Villare,F., Manetto,V., Chen,H.Y., Xue,R., Leal,S., Montagna,P., Cortelli,P., . (1992) Fatal familial insomnia, a prion disease with a mutation at codon 178 of the prion protein gene. *N. Engl. J. Med.*, **326**, 444-449.

4. Monari,L., Chen,S.G., Brown,P., Parchi,P., Petersen,R.B., Mikol,J., Gray,F., Cortelli,P., Montagna,P., Ghetti,B., . (1994) Fatal familial insomnia and familial Creutzfeldt-Jakob disease: different prion proteins determined by a DNA polymorphism. *Proc. Natl. Acad. Sci. U. S. A*, **91**, 2839-2842.

5. Montagna,P., Gambetti,P., Cortelli,P., Lugaresi,E. (2003) Familial and sporadic fatal insomnia. *Lancet Neurol.*, **2**, 167-176.

6. Krasnianski,A., Bartl,M., Sanchez Juan,P.J., Heinemann,U., Meissner,B., Varges,D., Schulze-Sturm,U., Kretzschmar,H.A., Schulz-Schaeffer,W.J., Zerr,I. (2008) Fatal familial insomnia: Clinical features and early identification. *Ann. Neurol.*, **63**, 658-661.

7. Lugaresi,E., Medori,R., Montagna,P., Baruzzi,A., Cortelli,P., Lugaresi,A., Tinuper,P., Zucconi,M., Gambetti,P. (1986) Fatal familial insomnia and dysautonomia with selective degeneration of thalamic nuclei. *N. Engl. J. Med.*, **315**, 997-1003.

8. Gallassi,R., Morreale,A., Montagna,P., Cortelli,P., Avoni,P., Castellani,R., Gambetti,P., Lugaresi,E. (1996) Fatal familial insomnia: behavioral and cognitive features. *Neurology*, **46**, 935-939.

9. Cortelli,P., Gambetti,P., Montagna,P., Lugaresi,E. (1999) Fatal familial insomnia: clinical features and molecular genetics. *J. Sleep Res.*, **8 Suppl 1**, 23-29.

10. Gambetti,P., Parchi,P., Petersen,R.B., Chen,S.G., Lugaresi,E. (1995) Fatal familial insomnia and familial Creutzfeldt-Jakob disease: clinical, pathological and molecular features. *Brain Pathol.*, **5**, 43-51.

11. Gambetti,P., Parchi,P., Chen,S.G. (2003) Hereditary Creutzfeldt-Jakob disease and fatal familial insomnia. *Clin. Lab Med.*, **23**, 43-64.

12. Cortelli,P., Perani,D., Parchi,P., Grassi,F., Montagna,P., De,M.M., Castellani,R., Tinuper,P., Gambetti,P., Lugaresi,E., Fazio,F. (1997) Cerebral metabolism in fatal familial insomnia: relation to duration, neuropathology, and distribution of protease-resistant prion protein. *Neurology*, **49**, 126-133.

13. Cortelli,P., Gambetti,P., Montagna,P., Lugaresi,E. (1999) Fatal familial insomnia: clinical features and molecular genetics. *J. Sleep Res.*, **8 Suppl 1**, 23-29.

14. Schenkein,J., Montagna,P. (2006) Self management of fatal familial insomnia. Part 1: what is FFI? *MedGenMed.*, **8**, 65.

15. Manetto,V., Medori,R., Cortelli,P., Montagna,P., Tinuper,P., Baruzzi,A., Rancurel,G., Hauw,J.J., Vanderhaeghen,J.J., Mailleux,P., . (1992) Fatal familial insomnia: clinical and pathologic study of five new cases. *Neurology*, **42**, 312-319.

16. Cortelli,P., Perani,D., Montagna,P., Gallassi,R., Tinuper,P., Provini,F., Avoni,P., Ferrillo,F., Anchisi,D., Moresco,R.M.*, et al.* (2006) Pre-symptomatic diagnosis in fatal familial insomnia: serial neurophysiological and 18FDG-PET studies. *Brain*, **129**, 668-675.

17. Parchi,P., Castellani,R., Cortelli,P., Montagna,P., Chen,S.G., Petersen,R.B., Manetto,V., Vnencak-Jones,C.L., McLean,M.J., Sheller,J.R., . (1995) Regional distribution of protease-resistant prion protein in fatal familial insomnia. *Ann. Neurol.*, **38**, 21-29.

18. Xie,W.L., Shi,Q., Xia,S.L., Zhang,B.Y., Gong,H.S., Wang,S.B., Xu,Y., Guo,Y., Tian,C., Zhang,J.*, et al.* (2013) Comparison of the pathologic and pathogenic features in six different regions of postmortem brains of three patients with fatal familial insomnia. *Int. J. Mol. Med.*, **31**, 81-90.

19. Tabernero,C., Polo,J.M., Sevillano,M.D., Munoz,R., Berciano,J., Cabello,A., Baez,B., Ricoy,J.R., Carpizo,R., Figols,J.*, et al.* (2000) Fatal familial insomnia: clinical, neuropathological, and genetic description of a Spanish family. *J. Neurol. Neurosurg. Psychiatry*, **68**, 774-777.

20. Shi,Q., Xie,W.L., Zhang,B., Chen,L.N., Xu,Y., Wang,K., Ren,K., Zhang,X.M., Chen,C., Zhang,J., Dong,X.P. (2013) Brain microglia were activated in sporadic CJD but almost unchanged in fatal familial insomnia and G114V genetic CJD. *Virol. J.*, **10**, 216.

21. Dorandeu,A., Wingertsmann,L., Chretien,F., Delisle,M.B., Vital,C., Parchi,P., Montagna,P., Lugaresi,E., Ironside,J.W., Budka,H.*, et al.* (1998) Neuronal apoptosis in fatal familial insomnia. *Brain Pathol.*, **8**, 531-537.

22. Tian,C., Liu,D., Xiang,W., Kretzschmar,H.A., Sun,Q.L., Gao,C., Xu,Y., Wang,H., Fan,X.Y., Meng,G.*, et al.* (2014) Analyses of the similarity and difference of global gene expression profiles in cortex regions of three neurodegenerative diseases: sporadic Creutzfeldt-Jakob disease (sCJD), fatal familial insomnia (FFI), and Alzheimer's disease (AD). *Mol. Neurobiol.*, **50**, 473-481.

23. Tian,C., Liu,D., Sun,Q.L., Chen,C., Xu,Y., Wang,H., Xiang,W., Kretzschmar,H.A., Li,W., Chen,C.*, et al.* (2013) Comparative analysis of gene expression profiles between cortex and thalamus in Chinese fatal familial insomnia patients. *Mol. Neurobiol.*, **48**, 36-48.

24. Shi,Q., Chen,L.N., Zhang,B.Y., Xiao,K., Zhou,W., Chen,C., Zhang,X.M., Tian,C., Gao,C., Wang,J.*, et al.* (2015) Proteomics analyses for the global proteins in the brain tissues of different human prion diseases. *Mol. Cell Proteomics.*, **14**, 854-869.

25. Bouybayoune,I., Mantovani,S., Del,G.F., Bertani,I., Restelli,E., Comerio,L., Tapella,L., Baracchi,F., Fernandez-Borges,N., Mangieri,M.*, et al.* (2015) Transgenic fatal familial insomnia mice indicate prion infectivity-independent mechanisms of pathogenesis and phenotypic expression of disease. *PLoS. Pathog.*, **11**, e1004796.

26. Jackson,W.S., Borkowski,A.W., Faas,H., Steele,A.D., King,O.D., Watson,N., Jasanoff,A., Lindquist,S. (2009) Spontaneous generation of prion infectivity in fatal familial insomnia knockin mice. *Neuron*, **63**, 438-450.

27. Silva,C.J. (2012) Using small molecule reagents to selectively modify epitopes based on their conformation. *Prion.*, **6**, 163-173.

28. Atarashi,R., Satoh,K., Sano,K., Fuse,T., Yamaguchi,N., Ishibashi,D., Matsubara,T., Nakagaki,T., Yamanaka,H., Shirabe,S.*, et al.* (2011) Ultrasensitive human prion detection in cerebrospinal fluid by real-time quaking-induced conversion. *Nat. Med.*, **17**, 175-178.

29. McGuire,L.I., Peden,A.H., Orru,C.D., Wilham,J.M., Appleford,N.E., Mallinson,G., Andrews,M., Head,M.W., Caughey,B., Will,R.G.*, et al.* (2012) Real time quaking-induced conversion analysis of cerebrospinal fluid in sporadic Creutzfeldt-Jakob disease. *Ann. Neurol.*, **72**, 278-285.

30. Peden,A.H., McGuire,L.I., Appleford,N.E., Mallinson,G., Wilham,J.M., Orru,C.D., Caughey,B., Ironside,J.W., Knight,R.S., Will,R.G.*, et al.* (2012) Sensitive and specific detection of sporadic Creutzfeldt-Jakob disease brain prion protein using real-time quaking-induced conversion. *J. Gen. Virol.*, **93**, 438-449.

31. Almer,G., Hainfellner,J.A., Brucke,T., Jellinger,K., Kleinert,R., Bayer,G., Windl,O., Kretzschmar,H.A., Hill,A., Sidle,K.*, et al.* (1999) Fatal familial insomnia: a new Austrian family. *Brain*, **122 (Pt 1)**, 5-16.

32. Ladogana,A., Sanchez-Juan,P., Mitrova,E., Green,A., Cuadrado-Corrales,N., Sanchez-Valle,R., Koscova,S., Aguzzi,A., Sklaviadis,T., Kulczycki,J.*, et al.* (2009) Cerebrospinal fluid biomarkers in human genetic transmissible spongiform encephalopathies. *J. Neurol.*, **256**, 1620-1628.

33. Le,D.A., Beringue,V., Andreoletti,O., Reine,F., Lai,T.L., Baron,T., Bratberg,B., Vilotte,J.L., Sarradin,P., Benestad,S.L., Laude,H. (2005) A newly identified type of scrapie agent can naturally infect sheep with resistant PrP genotypes. *Proc. Natl. Acad. Sci. U. S. A*, **102**, 16031-16036.

34. Parchi,P., Castellani,R., Cortelli,P., Montagna,P., Chen,S.G., Petersen,R.B., Manetto,V., Vnencak-Jones,C.L., McLean,M.J., Sheller,J.R., . (1995) Regional distribution of protease-resistant prion protein in fatal familial insomnia. *Ann. Neurol.*, **38**, 21-29.

35. Ferrer,I., Rivera,R., Blanco,R., Marti,E. (1999) Expression of proteins linked to exocytosis and neurotransmission in patients with Creutzfeldt-Jakob disease. *Neurobiol. Dis.*, **6**, 92-100.

36. Ferrer,I., Puig,B., Blanco,R., Marti,E. (2000) Prion protein deposition and abnormal synaptic protein expression in the cerebellum in Creutzfeldt-Jakob disease. *Neuroscience*, **97**, 715-726.

37. Jeffrey,M., McGovern,G., Siso,S., Gonzalez,L. (2011) Cellular and sub-cellular pathology of animal prion diseases: relationship between morphological changes, accumulation of abnormal prion protein and clinical disease. *Acta Neuropathol.*, **121**, 113-134.

38. Llorens,F., Lopez-Gonzalez,I., Thune,K., Carmona,M., Zafar,S., Andreoletti,O., Zerr,I., Ferrer,I. (2014) Subtype and regional-specific neuroinflammation in sporadic creutzfeldt-jakob disease. *Front Aging Neurosci.*, **6**, 198.

39. Kothari,P., Pestana,R., Mesraoua,R., Elchaki,R., Khan,K.M., Dannenberg,A.J., Falcone,D.J. (2014) IL-6-mediated induction of matrix metalloproteinase-9 is modulated by JAK-dependent IL-10 expression in macrophages. *J. Immunol.*, **192**, 349-357.

40. Kim,J.I., Ju,W.K., Choi,J.H., Choi,E., Carp,R.I., Wisniewski,H.M., Kim,Y.S. (1999) Expression of cytokine genes and increased nuclear factor-kappa B activity in the brains of scrapie-infected mice. *Brain Res. Mol. Brain Res.*, **73**, 17-27.

41. Kovacs,G.G., Budka,H. (2010) Distribution of apoptosis-related proteins in sporadic Creutzfeldt-Jakob disease. *Brain Res.*, **1323**, 192-199.

42. Pamplona,R., Naudi,A., Gavin,R., Pastrana,M.A., Sajnani,G., Ilieva,E.V., Del Rio,J.A., Portero-Otin,M., Ferrer,I., Requena,J.R. (2008) Increased oxidation, glycoxidation, and lipoxidation of brain proteins in prion disease. *Free Radic. Biol. Med.*, **45**, 1159-1166.

43. Choi,S.I., Ju,W.K., Choi,E.K., Kim,J., Lea,H.Z., Carp,R.I., Wisniewski,H.M., Kim,Y.S. (1998) Mitochondrial dysfunction induced by oxidative stress in the brains of hamsters infected with the 263 K scrapie agent. *Acta Neuropathol.*, **96**, 279-286.

44. Llorens,F., Ansoleaga,B., Garcia-Esparcia,P., Zafar,S., Grau-Rivera,O., Lopez-Gonzalez,I., Blanco,R., Carmona,M., Yague,J., Nos,C*., et al.* (2013) PrP mRNA and protein expression in brain and PrP(c) in CSF in Creutzfeldt-Jakob disease MM1 and VV2. *Prion.*, **7**, 383-393.

45. Hill,A.F., Joiner,S., Beck,J.A., Campbell,T.A., Dickinson,A., Poulter,M., Wadsworth,J.D., Collinge,J. (2006) Distinct glycoform ratios of protease resistant prion protein associated with PRNP point mutations. *Brain*, **129**, 676-685.

46. Collinge,J., Sidle,K.C., Meads,J., Ironside,J., Hill,A.F. (1996) Molecular analysis of prion strain variation and the aetiology of 'new variant' CJD. *Nature*, **383**, 685-690.

47. Xiao,X., Yuan,J., Haik,S., Cali,I., Zhan,Y., Moudjou,M., Li,B., Laplanche,J.L., Laude,H., Langeveld,J*., et al.* (2013) Glycoform-selective prion formation in sporadic and familial forms of prion disease. *PLoS. One.*, **8**, e58786.

48. Lawson,V.A., Collins,S.J., Masters,C.L., Hill,A.F. (2005) Prion protein glycosylation. *J. Neurochem.*, **93**, 793-801.

49. Winklhofer,K.F., Heller,U., Reintjes,A., Tatzelt,J. (2003) Inhibition of complex glycosylation increases the formation of PrPsc. *Traffic.*, **4**, 313-322.

50. Silveira,J.R., Raymond,G.J., Hughson,A.G., Race,R.E., Sim,V.L., Hayes,S.F., Caughey,B. (2005) The most infectious prion protein particles. *Nature*, **437**, 257-261.

51. Simoneau,S., Rezaei,H., Sales,N., Kaiser-Schulz,G., Lefebvre-Roque,M., Vidal,C., Fournier,J.G., Comte,J., Wopfner,F., Grosclaude,J*., et al.* (2007) In vitro and in vivo neurotoxicity of prion protein oligomers. *PLoS. Pathog.*, **3**, e125.

52. Huang,P., Lian,F., Wen,Y., Guo,C., Lin,D. (2013) Prion protein oligomer and its neurotoxicity. *Acta Biochim. Biophys. Sin. (Shanghai)*, **45**, 442-451.

53. Choi,Y.P., Peden,A.H., Groner,A., Ironside,J.W., Head,M.W. (2010) Distinct stability states of disease-associated human prion protein identified by conformation-dependent immunoassay. *J. Virol.*, **84**, 12030-12038.

54. Bieschke,J., Weber,P., Sarafoff,N., Beekes,M., Giese,A., Kretzschmar,H. (2004) Autocatalytic self-propagation of misfolded prion protein. *Proc. Natl. Acad. Sci. U. S. A*, **101**, 12207-12211.

55. Barron,R.M., Campbell,S.L., King,D., Bellon,A., Chapman,K.E., Williamson,R.A., Manson,J.C. (2007) High titers of transmissible spongiform encephalopathy infectivity associated with extremely low levels of PrPSc in vivo. *J. Biol. Chem.*, **282**, 35878-35886.

56. Riesner,D. (2003) Biochemistry and structure of PrP(C) and PrP(Sc). *Br. Med. Bull.*, **66**, 21-33.

57. Makarava,N., Kovacs,G.G., Savtchenko,R., Alexeeva,I., Ostapchenko,V.G., Budka,H., Rohwer,R.G., Baskakov,I.V. (2012) A new mechanism for transmissible prion diseases. *J. Neurosci.*, **32**, 7345-7355.

58. Fernandez-Borges,N., Erana,H., Elezgarai,S.R., Harrathi,C., Gayosso,M., Castilla,J. (2013) Infectivity versus Seeding in Neurodegenerative Diseases Sharing a Prion-Like Mechanism. *Int. J. Cell Biol.*, **2013**, 583498.

59. Rodriguez-Martinez,A.B., Alfonso-Sanchez,M.A., Pena,J.A., Sanchez-Valle,R., Zerr,I., Capellari,S., Calero,M., Zarranz,J.J., de Pancorbo,M.M. (2008) Molecular evidence of founder effects of fatal familial insomnia through SNP haplotypes around the D178N mutation. *Neurogenetics.*, **9**, 109-118.

60. Cramm,M., Schmitz,M., Karch,A., Mitrova,E., Kuhn,F., Schroeder,B., Raeber,A., Varges,D., Kim,Y.S., Satoh,K*., et al.* (2015) Stability and Reproducibility Underscore Utility of RT-QuIC for Diagnosis of Creutzfeldt-Jakob Disease. *Molecular Neurobiology*, 1-9.

61. Garcia-Esparcia,P., Llorens,F., Carmona,M., Ferrer,I. (2014) Complex deregulation and expression of cytokines and mediators of the immune response in Parkinson's disease brain is region dependent. *Brain Pathol.*, **24**, 584-598.

Legends to Figures

Figure 1: Neuropathological assays of the Thalamus, Cerebellum and Entorhinal Cortex of FFI cases. Left: Hematoxylin and eosin staining. Right: Nissl staining.

Figure 2: Expression of synaptic and neuronal markers in the thalamus, cerebellum and entorhinal cortex in FFI and control cases: A) Western blotting analyses of PSD-95, synapsin, synaptophysin, 14-3-3 γ, β and ε subunits, NeuN, NF-L, Tau (total Tau, Tau-5) and p-Tau (T181) in the thalamus, cerebellum and entorhinal cortex in five control and FFI representative cases. B) Densitometry from all the cases analysed by western blotting using GAPDH and β-actin for normalisation. Coomassie blue was used to control total protein loading. C) Tau mRNA expression in the thalamus and entorhinal cortex in control and FFI samples were normalised using XPNPEP1 as determined by TaqMan PCR assays; * $p<0.05$; ** $p<0.01$; *** $p<0.001$.

Figure 3: Astroglia and microglia in the thalamus, cerebellum and entorhinal cortex in FFI: A) mRNA expression of microglial markers Iba-1/Aif-1, Cd68 and Cd11b; astroglial marker GFAP; dual microglial/astroglial activator CNTF; and oligodendrocyte marker Olig2 expression in the thalamus (upper panel) and entorhinal cortex (lower panel) in control and FFI samples as determined by TaqMan PCR assays. Values are normalised using XPNPEP1. GFAP mRNA expression was increased in the thalamus and entorhinal cortex in FFI. Two cases show an apparent increase in microglia cell markers in the thalamus. B) Immunohistochemistry shows increased GFAP-immunoreactive astrocytes in the thalamus and entorhinal cortex, but not in the cerebellum, in FFI. No increased numbers of Iba-1-immunoreactive cells are observed in the thalamus, entorhinal cortex or cerebellum in FFI, but the morphology of microglia differs in the thalamus, and particularly in the entorhinal cortex, in FFI. Paraffin sections, slight hematoxylin counterstaining. C) GFAP, but not Iba-1 protein expression levels are significantly increased in the thalamus, entorhinal cortex and cerebellum in FFI. Student's t test: *$p<0.05$; ***$p<0.001$.

Figure 4: Neuroinflammatory mediators in the thalamus and entorhinal cortex in FFI: A) Increased IL6 mRNA expression in the thalamus validated with two housekeeping genes GAPDH and GUSB. B) IL6 immunoreactivity is expressed in microglia in the entorhinal cortex and the thalamus in

FFI; paraffin sections slightly counterstained with hematoxylin. C) Western blot analyses of IkBα, SOD-1 and COX-2 in the thalamus, cerebellum and entorhinal cortex in control and FFI cases. Five representative cases per group and brain region are shown. GAPDH was used for normalisation. Densitometry from all the cases analysed by Western blot: (C) mRNA expression of I6 in the thalamus of control and FFI samples as determined by TaqMan PCR assays. Values were normalised using GAPDH and GUSB as internal controls (housekeeping genes) showing similar differences between groups. Student's t test: * $p<0.05$, ** $p<0.01$.

Figure 5: PrP expression in the thalamus, cerebellum and entorhinal cortex in FFI: A) Localization of PrP sites recognised by the anti-PrP antibodies used in the analysis referring to the sequence and domains of the PrP protein. SP: signal peptide; CC1 and CC2: charged clusters; HC: hydrophobic core; H1, H2, and H3: helix 1, helix 2 and helix 3; S-S: disulphide bridge; GPI: glycophosphatidylinositol anchor. B) Western blot analyses with anti-PrP antibodies SAF32, 3F4, SAF61, 12F10 and 8H4 in the thalamus, cerebellum and entorhinal cortex in control and FFI cases. Seven representative cases per group and brain region are shown; GAPDH and β-actin are used for normalisation. Densitometry from all cases analysed by Western blot shows a significant region-dependent decrease of PrP immunoreactivity but increased SAF61 and 12F10 immunoreactivity of the band of about 19 kDa in the thalamus, but not in other brain regions, in FFI. C) mRNA expression of PrP in the thalamus and entorhinal cortex of control and FFI determined by TaqMan PCR assays. Values normalised using GAPDH and GUSB as internal controls show decreased expression in the thalamus and entorhinal cortex in FFI compared with controls. Student's t test: *$p<0.05$; **$p<0.01$; ***$p<0.001$.

Figure 6: PK-resistant PrP (PrPres) in the thalamus, cerebellum and entorhinal cortex in FFI: A) Brain homogenates of FFI cases digested with proteinase K (PK9) at the indicated concentrations and processed for Western blotting using the SAF70 antibody show a strong signal for the diglycosylated band, a weaker signal for the monoglycosylated band, and a faint signal for the nonglycosylated band in the entorhinal cortex of FFI cases (lanes 1, 2, 5 and 6), in comparison to the lack of PrPres in the entorhinal cortex in controls (lanes 3, 4, 7 and 8). B) No PrPres immunoreactivity

is detected in the thalamus processed in parallel with the positive PrP synaptic pattern of PrPres in the entorhinal cortex in FFI; paraffin sections, 3F4 antibody, slight hematoxylin counterstaining.

Figure 7: Detection of abnormal PrP in the thalamus and entorhinal cortex in FFI: A) Dot blot analysis of PrP levels in the thalamus and entorhinal cortex of control and FFI cases (three representative cases), and in the cerebellum of one control and one sCJD MM1 case using the anti-PrPsc conformational antibody 15B3. Densitometries of five cases for each group of samples are shown in the accompanying graph (EC: entorhinal cortex, T: thalamus, CB: cerebellum). Increased expression of altered PrP conformation is found in the entorhinal cortex in FFI in contrast with the weak expression in the thalamus. Strong immunoreactivity is observed in the cerebellum of a typical sCJD MM1 case. Student's t test: **$p<0.01$; ***$p<0.001$: comparison between control and FFI cases. # $p<0.05$: comparison between thalamus and entorhinal cortex. B) Western blotting of PrP in the thalamus and entorhinal cortex in control and FFI cases, and in the frontal cortex of one control and one sCJD MM1 case used for comparison. Brain homogenates were untreated (-) or treated (+) with Ac-NHS. Following treatment a large amount of PrP is present in sCJD whereas only a very small amount is in the entorhinal cortex and there is no signal in the thalamus in FFI.

Figure 8: Detection of insoluble PrP, oligomers and amyloid aggregates in the thalamus and entorhinal cortex of FFI cases: A) Western blotting analysis of PrP solubility and aggregation assays in the thalamus and entorhinal cortex in control and FFI cases and in the cerebellum of controls and sCJD cases. S2: cytosolic fraction, S3: deoxycholate-soluble fraction, S4: SDS-soluble fraction. Representative images for each group are shown and quantifications of three cases for each group are presented in the accompanying graph. Decreased levels in the cytosolic fraction and increased PrP levels in the insoluble fraction are seen in the thalamus and cerebellum in FFI cases compared with controls. The same pattern is observed in one sCJD case used as a positive control. B) Dot blot analysis of oligomers in the thalamus of control and FFI cases (3 representative cases) and in the cerebellum of one control and one sCJD MM1 case using the anti-oligomer conformational antibody 11A shows increased immunoreactivity in FFI and particularly in sCJD. C) Densitometry of the fluorescence in brain homogenates incubated with thioflavin T (ThT) in the thalamus, entorhinal cortex and cerebellum in FFI and in the cerebellum in sCJD MM1. A maximal increase was observed

in the cerebellum in sCJD, but a lower significant increase was also observed in the entorhinal cortex in FFI; Student's t test, *p<0.05; **p<0.01; ***p<0.001.

Figure 9: Differential prion seeding activity in the thalamus, cerebellum and entorhinal cortex in FFI. A) Prion seeding efficiency detected by RT-QuIC in the thalamus, cerebellum and entorhinal cortex in FFI cases (10^{-8} dilutions form 10% w/v brain homogenates). Control cases of the same brain regions were negative for prion seeding activity. RT-QuIC responses of all groups were measured in relative fluorescence units (RFU) for 80 hours. Samples reaching plateau indicate maximal fluorescence (60.000 RFU units). Characteristic curves for each case are shown. Three of seven, eight of eight and two of eight samples of the thalamus, entorhinal cortex and cerebellum, respectively, showed seeding activity. B) Correlation between RT-QuIC and PrP signal in the entorhinal cortex of FFI cases: PrPres values were obtained from densitometries of PK-digested PrP western-blots; total PrP values were obtained from densitometries of western-blots using SAF70 antibody. R value (Pearson correlation) and p value are indicated when statistically significant.

Figure 10: Prion seeding activity in pathologically affected regions of FFI and sCJD cases: A) Prion seeding efficiency detected by RT-QuIC in the thalamus, cerebellum and entorhinal cortex of FFI cases and in the frontal cortex (MM1) and cerebellum (VV2) of sCJD cases (10^{-6} dilutions from 10% w/v brain homogenates). Control cases of the same brain regions were negative for prion seeding activity. RT-QuIC responses of all groups were measured in relative fluorescence units (RFU) over a period of 100 h. The fluorescence plateau was determined to be 60.000 RFU units. B) Quantification of the RT-QuIC signal by means of AUC calculation. Five cases for each brain region (thalamus, cerebellum and entorhinal cortex for FFI cases and frontal cortex, and cerebellum for sCJD) were analysed. C) Quantification of the RT-QuIC signal by means of lag phase (in hours). Five cases for each brain region (thalamus, cerebellum and entorhinal cortex for FFI cases, and frontal cortex and cerebellum for sCJD) were analysed. ANOVA test followed by Tukey's Multiple-Comparison post hoc test revealed decreased AUC and increased lag phase in the cerebellum of FFI cases when compared with the rest of the groups. Values are expressed as mean ± SD. Values considered significant are represented as ** $p < 0.01$ and *** $p < 0.001$.

Table 1: mRNA expression of selected cytokines and mediators of the inflammatory response in the thalamus and entorhinal cortex in FFI: Data are represented as the mean ± SEM; XPNPEP1 is used as a housekeeping gene. Increased expression of interleukin 6 (IL6), interleukin 10 receptor alpha subunit (IL10RA), colony stimulating factor 3 receptor (CSF3R) and toll-like receptor 7 (TLR7) is observed in the thalamus in FFI, whereas interleukin 10 (IL10) is downregulated in the entorhinal cortex in FFI compared with controls. Student's t test: * $p<0.05$, ** $p<0.01$.

Supplementary Table 1: Summary of cases Age in years, post mortem delay (PMD in hours) and gender are indicated.

Supplementary Table 2: List of the Taqman probes

Supplementary Table 3: Summary of regional-dependent alterations in FFI

Table 1

A

THALAMUS	Probe	Control	FFI	Control vs FFI (p value)	
Pro-inflammatory cytokines	*IL1B*	1.097 ± 0.492	1.373 ± 1.137	0.594	-
	IL6	1.077 ± 0.434	4.304 ± 3.879	0.048	*
	IL6ST	1.008 ± 0.140	1.393 ± 0.578	0.111	-
	TNFRSF1	1.023 ± 0.237	2.252 ± 1.102	0.013	*
Anti-inflammatory cytokines	*IL10*	1.225 ± 0.870	0.876 ± 0.464	0.375	-
	IL10RA	1.036 ± 0.281	3.844 ± 1.868	0.004	**
	IL10RB	1.027 ± 0.240	1.220 ± 0.368	0.258	-
	TGFB1	1.049 ± 0.360	1.744 ± 0.856	0.711	-
	TGFB2	1.064 ± 0.400	1.959 ± 0.953	0.038	*
Complement system	*C1QL1*	1.120 ± 0.539	2.082 ± 1.462	0.132	-
	C1QTNF7	1.025 ± 0.250	2.702 ± 2.801	0.955	-
Colony stimulating factors	*CSF1R*	1.087 ± 0.451	1.601 ± 0.558	0.074	-
	CSF3R	1.011 ± 0.168	2.381 ± 1.045	0.009	**
Cathepsins	*CTSS*	1.066 ± 0.420	1.385 ± 0.619	0.272	-
Toll-like receptors	*TLR4*	1.063 ± 0.352	1.275 ± 0.433	0.349	-
	TLR7	1.097 ± 0.518	2.169 ± 1.058	0.030	*

B

ENTORHINAL CORTEX	Probe	Control	FFI	Control vs FFI (p value)	
Pro-inflammatory cytokines	*IL1B*	1.114 ± 0.582	1.350 ± 0.802	0.555	-
	IL6	1.576 ± 1.446	0.657 ± 0.576	0.221	-
	IL6ST	1.006 ± 0.117	1.055 ± 0.361	0.737	-
	TNFRSF1	1.158 ± 0.697	1.597 ± 0.897	0.315	-
Anti-inflammatory cytokines	*IL10*	1.126 ± 0.360	0.646 ± 0.168	0.010	*
	IL10RA	1.072 ± 0.444	1.095 ± 0.380	0.924	-
	IL10RB	1.079 ± 0.425	0.920 ± 0.370	0.450	-
	TGFB1	1.051 ± 0.338	0.959 ± 0.393	0.649	-
	TGFB2	1.009 ± 0.144	1.441 ± 0.734	0.151	-
Complement system	*C1QL1*	1.041 ± 0.286	1.160 ± 0.399	0.523	-
	C1QTNF7	1.027 ± 0.746	0.245 ± 0.357	0.125	-
	C3AR1	1.096 ± 0.510	0.891 ± 0.401	0.400	-
Colony stimulating factors	*CSF1R*	1.212 ± 0.830	0.654 ± 0.289	0.100	-
	CSF3R	1.064 ± 0.355	1.029 ± 0.603	0.903	-
Cathepsins	*CTSS*	1.081 ± 0.498	0.795 ± 0.466	0.271	-
Toll-like receptors	*TLR4*	1.052 ± 0.357	1.020 ± 0.539	0.896	-
	TLR7	1.234 ± 0.908	1.122 ± 0.511	0.768	-

Abbreviations

FFI: Fatal Familial Insomnia, PrPres: PrP resistant to proteinase K digestion, PrPsc: Scrapie PrP (abnormal and pathogenic PrP).

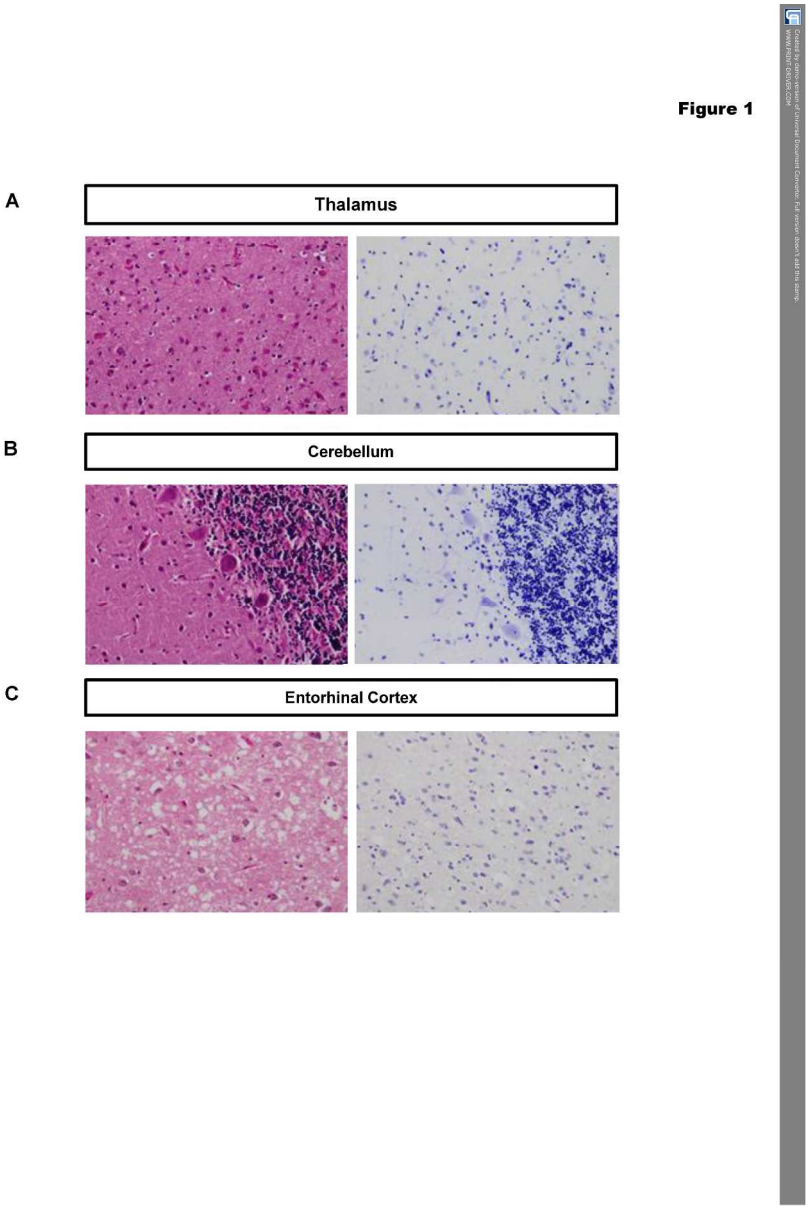

Figure 1: Neuropathological assays of the Thalamus, Cerebellum and Entorhinal Cortex of FFI cases.
297x420mm (300 x 300 DPI)

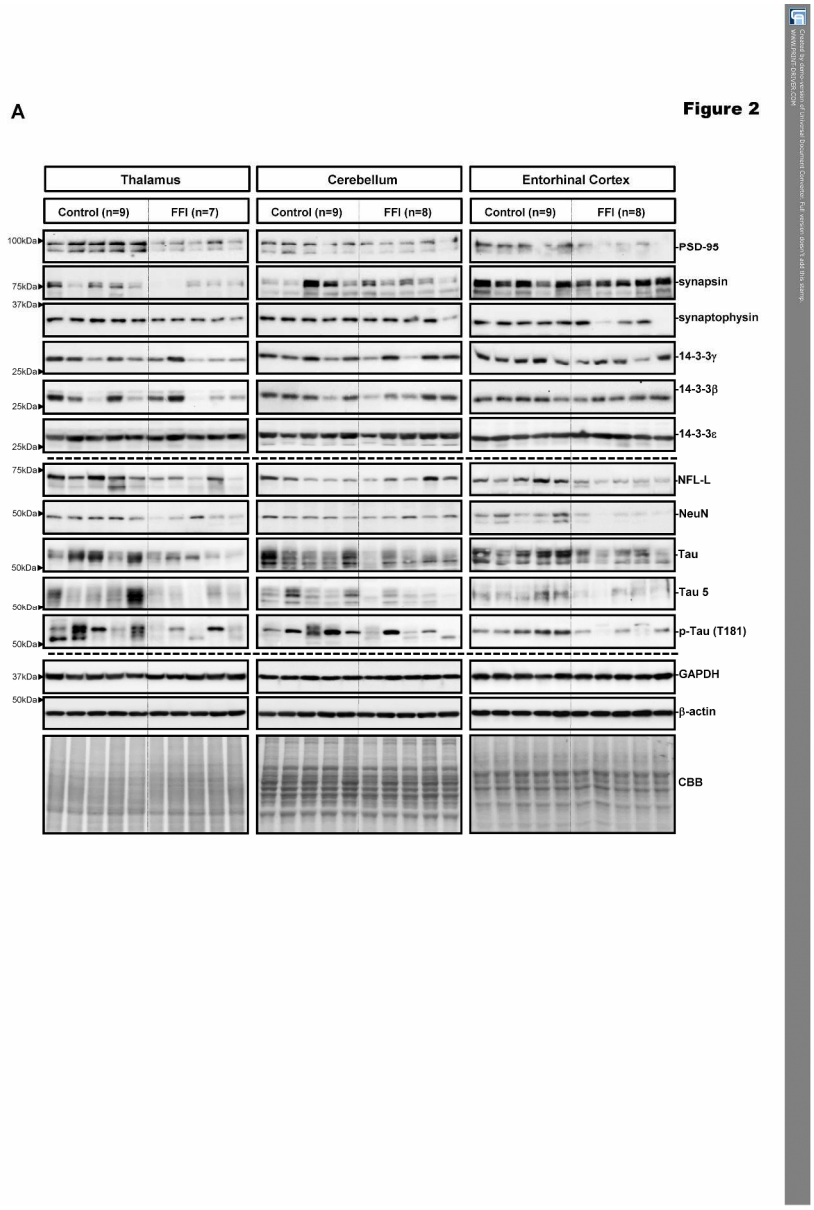

Expression of synaptic and neuronal markers in the thalamus, cerebellum and entorhinal cortex in FFI and control cases
297x420mm (300 x 300 DPI)

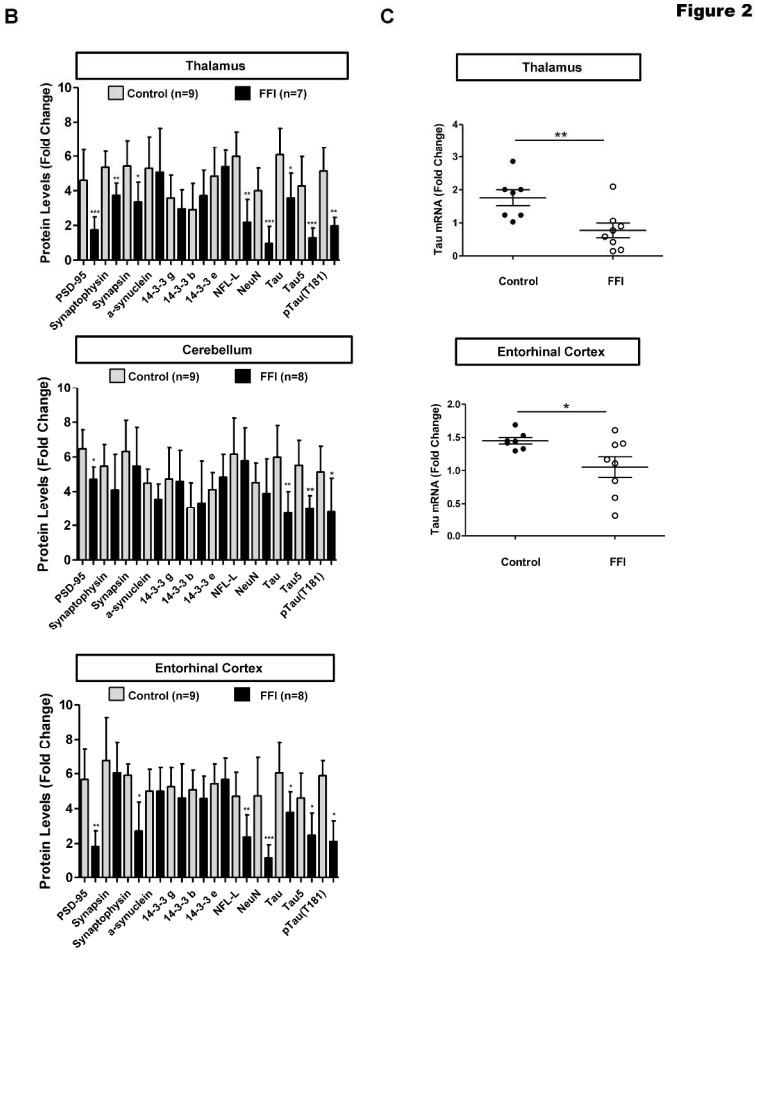

Expression of synaptic and neuronal markers in the thalamus, cerebellum and entorhinal cortex in FFI and control cases
297x420mm (300 x 300 DPI)

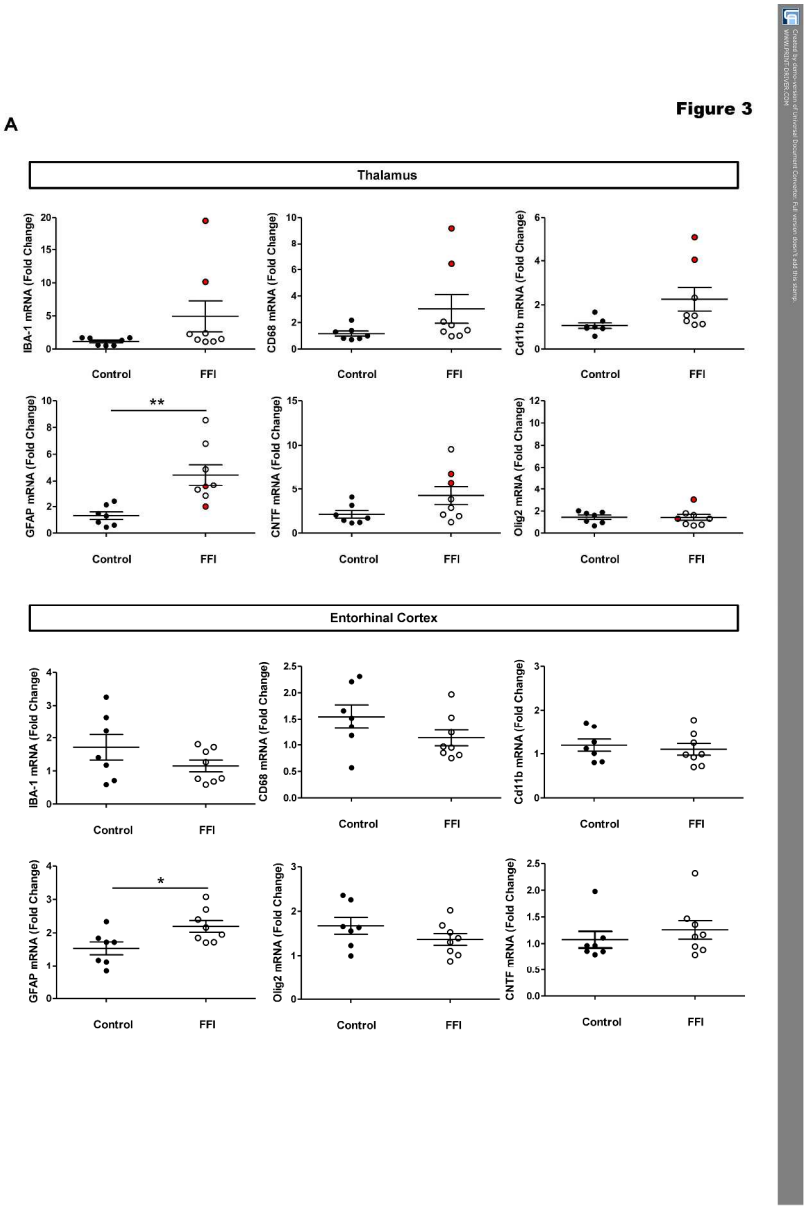

Astroglia and microglia in the thalamus, cerebellum and entorhinal cortex in FFI
297x420mm (300 x 300 DPI)

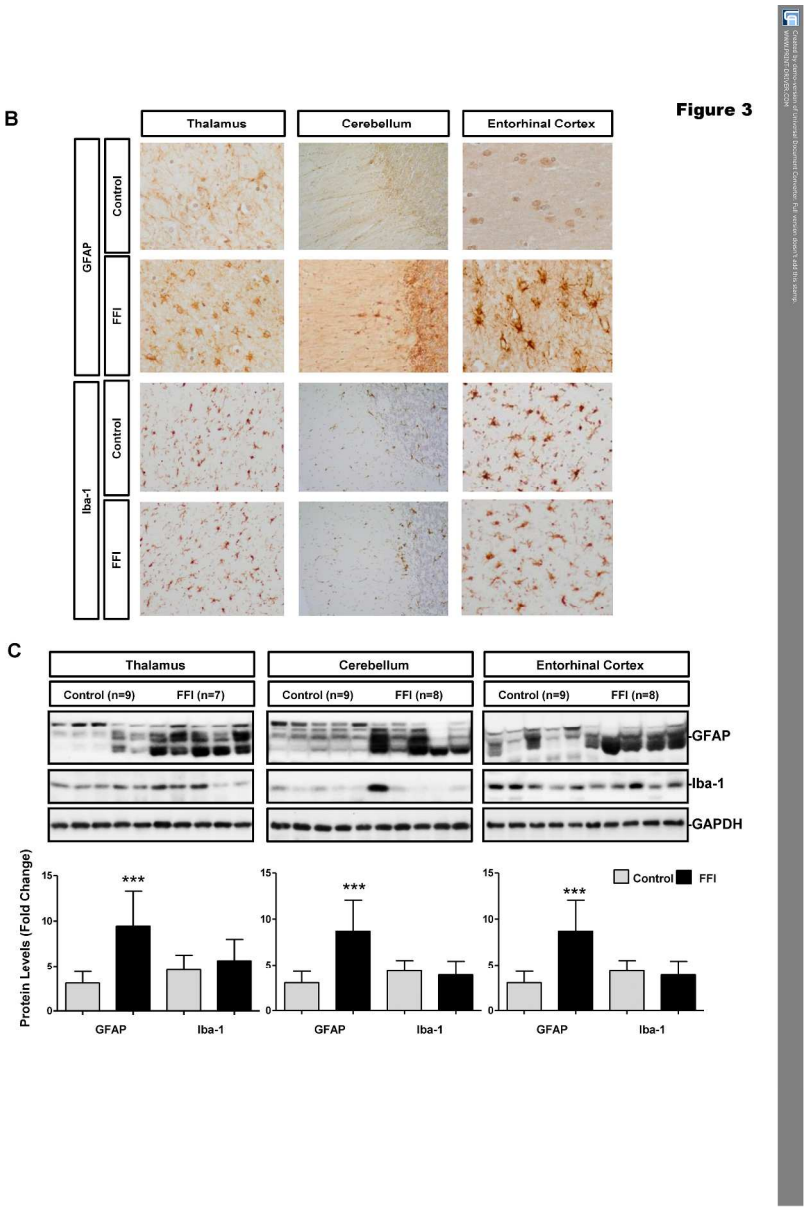

Astroglia and microglia in the thalamus, cerebellum and entorhinal cortex in FFI
297x420mm (300 x 300 DPI)

Figure 4

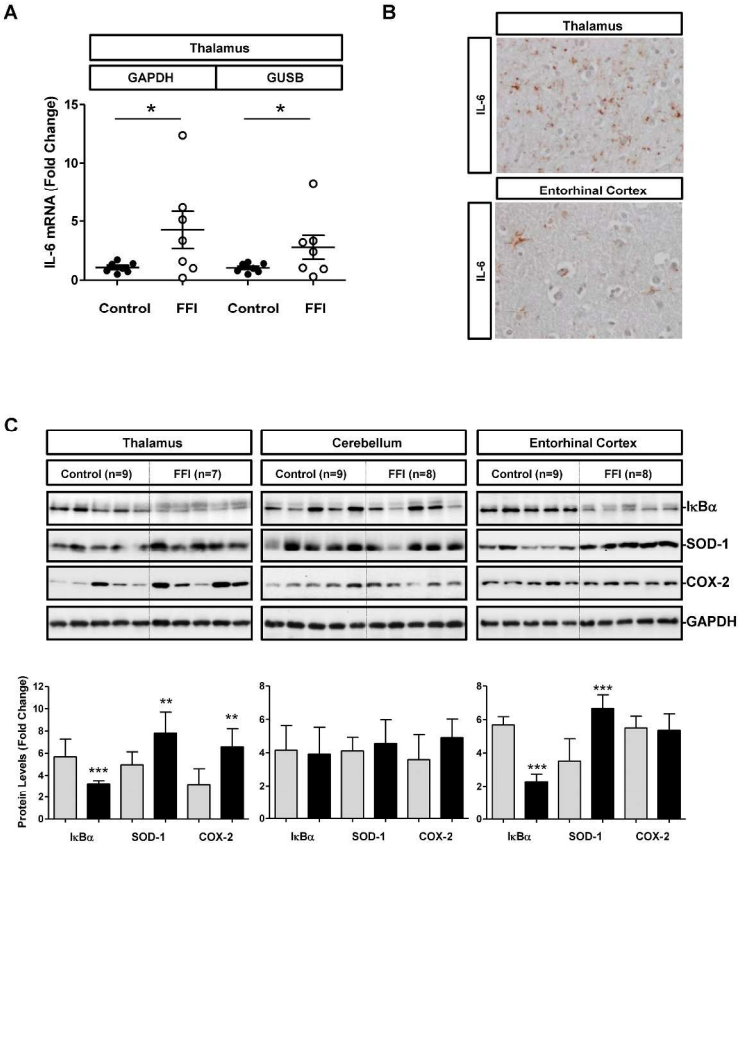

Neuroinflammatory mediators in the thalamus and entorhinal cortex in FFI
297x420mm (300 x 300 DPI)

Figure 5

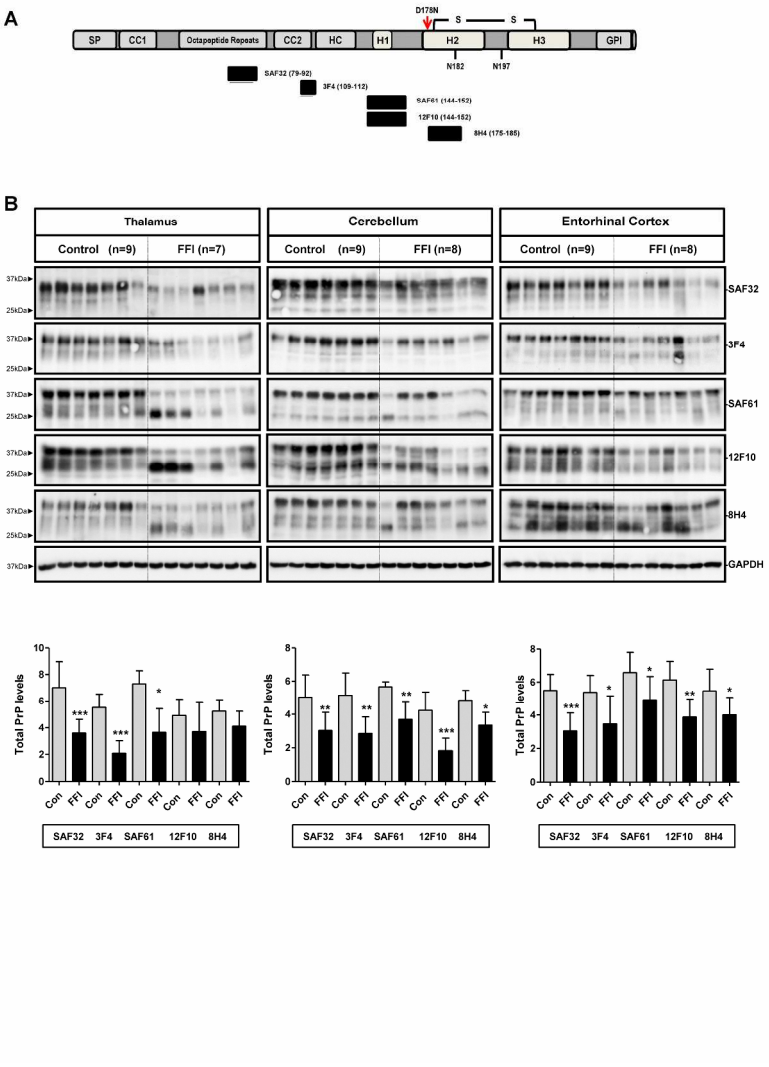

PrP expression in the thalamus, cerebellum and entorhinal cortex in FFI
297x420mm (300 x 300 DPI)

Figure 5

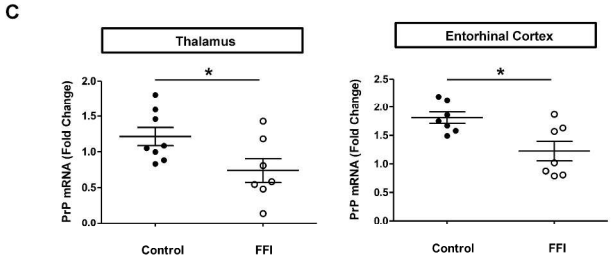

PrP expression in the thalamus, cerebellum and entorhinal cortex in FFI
297x420mm (300 x 300 DPI)

Figure 6

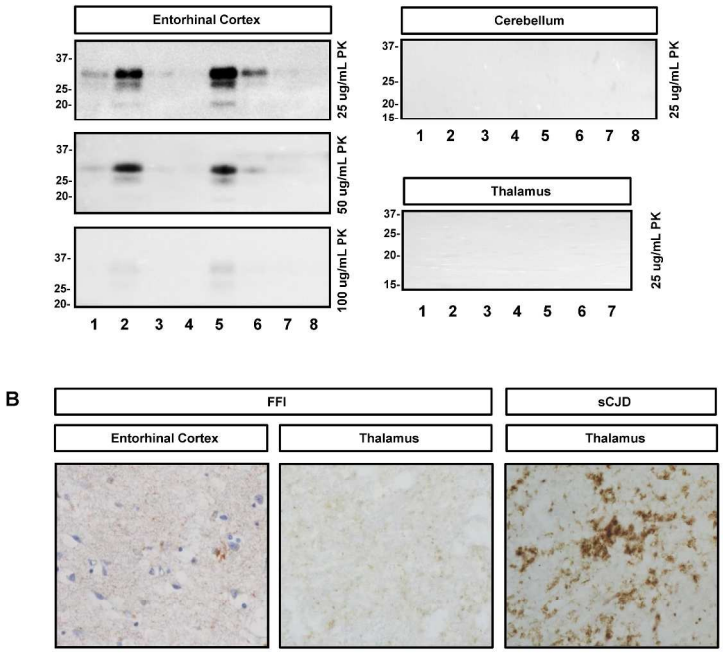

PK-resistant PrP (PrPres) in the thalamus, cerebellum and entorhinal cortex in FFI
297x420mm (300 x 300 DPI)

Figure 7

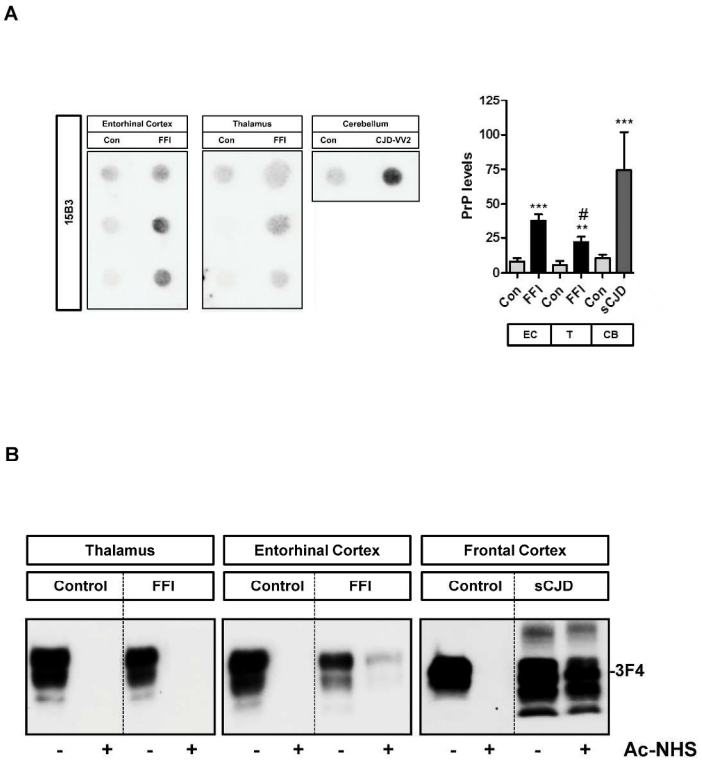

Detection of abnormal PrP in the thalamus and entorhinal cortex in FFI
297x420mm (300 x 300 DPI)

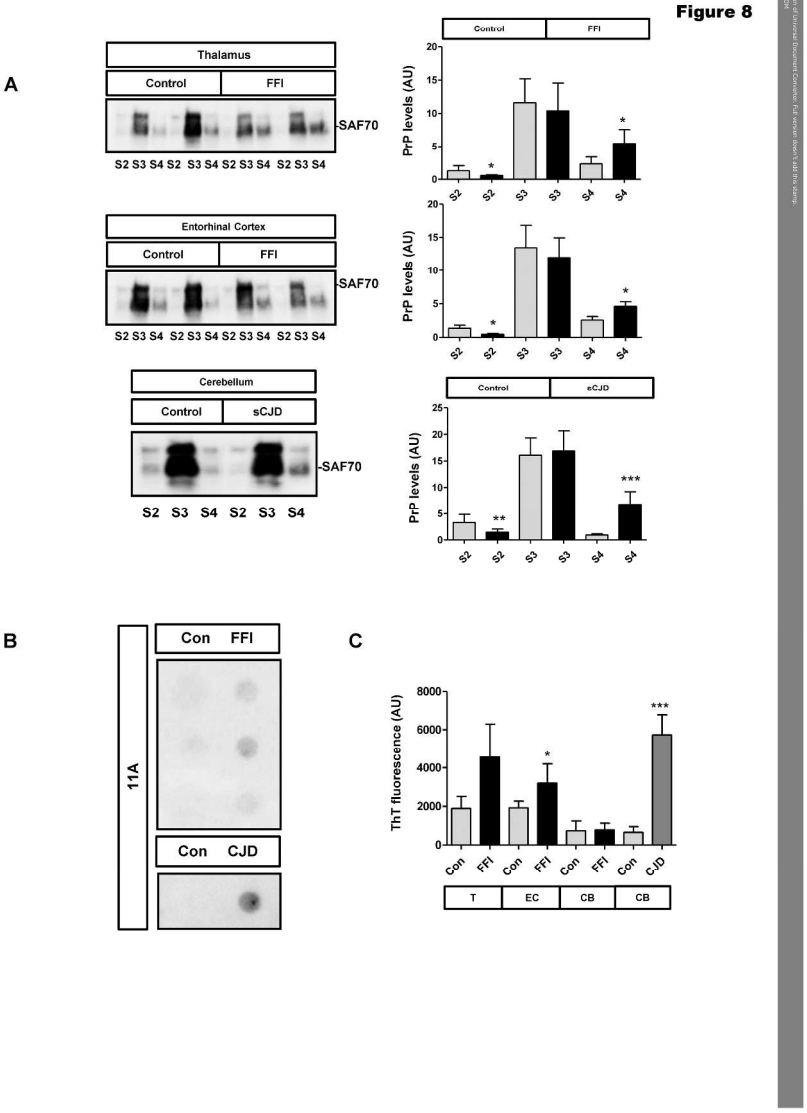

Detection of insoluble PrP, oligomers and amyloid aggregates in the thalamus and entorhinal cortex of FFI cases
297x420mm (300 x 300 DPI)

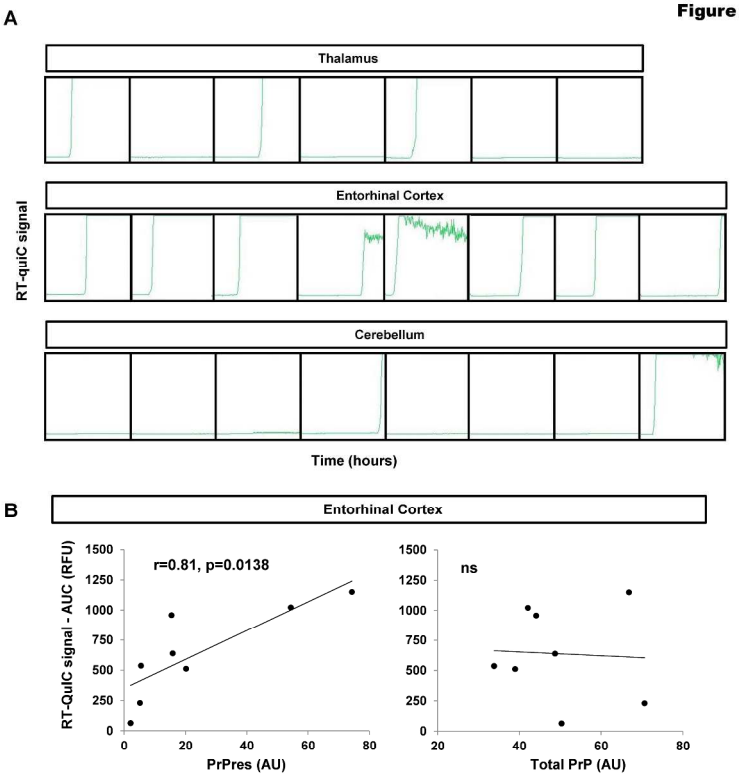

Figure 9

Differential prion seeding activity in the thalamus, cerebellum and entorhinal cortex in FFI
297x420mm (300 x 300 DPI)

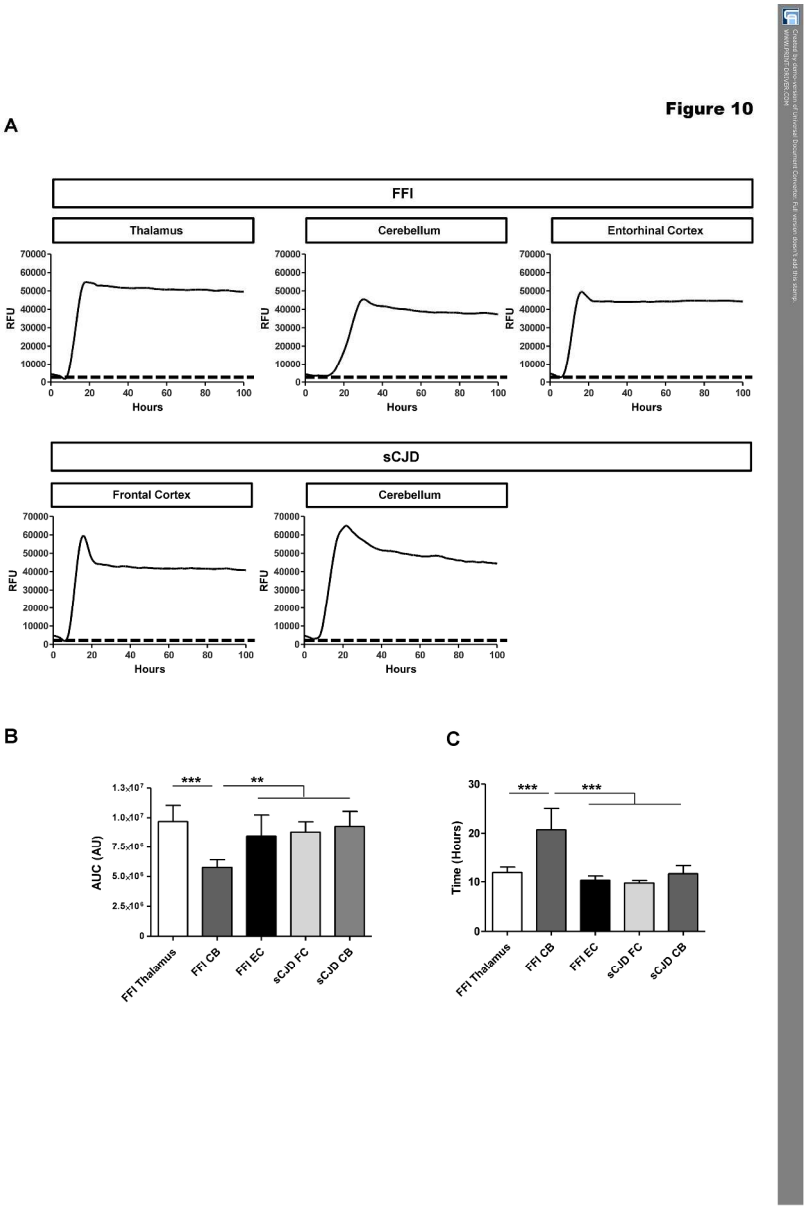

Prion seeding activity in pathologically affected regions of FFI and sCJD cases
297x420mm (300 x 300 DPI)